Searching for Galileo

by Mark L. Psiaki, Todd E. Humphreys, Shan Mohiuddin, Steven P. Powell, Alessandro P. Cerruti, and Paul M. Kintner, Jr.
Cornell University, Ithaca, N.Y., 14853-7501, U.S.A.

BIOGRAPHIES

Mark L. Psiaki is a Professor in the Sibley School of Mechanical and Aerospace Engineering. He received a B.A. in Physics and M.A. and Ph.D. degrees in Mechanical and Aerospace Engineering from Princeton University. His research interests are in the areas of estimation and filtering, spacecraft attitude and orbit determination, and GNSS technology and applications.

Todd E. Humphreys is a graduate student in the Sibley School of Mechanical and Aerospace Engineering. He received his B.S. and M.S. degrees in Electrical and Computer Engineering from Utah State University. His research interests are in estimation and filtering, spacecraft attitude determination, GNSS technology, and GNSS-based study of the ionosphere and neutral atmosphere.

Shan Mohiuddin is a graduate student in the Sibley School of Mechanical and Aerospace Engineering. He received a B.S. in Aerospace Engineering from Virginia Tech in 2003. He spent the summer of 2003 working in the Flight Dynamics Analysis Branch at the NASA/Goddard Space Flight Center. His research focuses on developing estimation techniques for precise spacecraft relative navigation, on general GNSS data processing algorithms, and on GNSS receiver design.

Steven P. Powell is a Senior Engineer with the Space Plasma Physics Group in the Department of Electrical and Computer Engineering. He has M.S. and B.S. degrees in Electrical Engineering from Cornell University. He has been involved with the design, fabrication, and testing of several GNSS receivers.

Alessandro P. Cerruti is currently a Ph.D. candidate with the Space Physics and Engineering Group in the School of Electrical and Computer Engineering. His primary interest is space weather and its effects on GNSS receiver operation.

Paul M. Kintner, Jr. is a Professor of Electrical and Computer Engineering. He received a B.S in Physics from the University of Rochester and a Ph.D. in Physics from the University of Minnesota. His research interests include the electrical properties of upper atmospheres, space weather, and developing GNSS instruments for space science. He is a Fellow of the APS.

ABSTRACT

Statistical analysis techniques have been used to find and decode the L1 BOC(1,1) signal of the first prototype Galileo spacecraft, GIOVE-A. The resulting pseudo-random number (PRN) codes can be used by receiver developers to test their devices on the GIOVE-A signals. The analysis has used codeless techniques to acquire the signal and to remove its carrier and binary offset carrier (BOC) components, and it has determined the timing and chip values of the PRN codes using optimal statistical signal processing methods. The resulting codes' per-chip error probabilities are less than 10^{-10}. The period of the pilot PRN code is 200 ms, which is twice the length published in Galileo documentation.

INTRODUCTION

Galileo, Europe's answer to the U.S. GPS system, achieved a milestone on 28 December 2005 with the launch of its first test satellite, GIOVE-A, which began transmitting navigation signals in early January 2006. After the launch, receiver developers around the world were anxious to test their Galileo-capable receivers on the GIOVE-A signals. Because the Galileo signal structure documentation had not yet been finalized, however, only approved groups involved in validation tests were provided the PRN codes required to track the GIOVE-A navigation signals.

Eager to study the Galileo signals and to develop Galileo-capable receivers, the authors set out to determine whether the GIOVE-A L1 BOC(1,1) signal could be acquired and the PRN codes uncovered using codeless acquisition and statistical signal processing techniques. The short answer: Yes!

Data were recorded using a digital storage receiver connected to an inexpensive roof-mounted patch antenna on Cornell University's campus in Ithaca, NY. The data were then processed off-line in several stages. A schematic diagram of the data collection and analysis system is shown in Fig. 1. In the first step of the processing, the nuisance GPS and SBAS C/A-code signals were tracked and removed. The second step was to determine the GIOVE-A L1 BOC(1,1) signal's carrier phase, Doppler shift, and BOC phase using codeless acquisition techniques. Next, the carrier and BOC signals were removed by mixing, and 1.023-MHz in-phase

Preprint from ION GNSS 2006

accumulations were computed. Finally, the code timing, data symbols, and secondary code chips were analyzed, and the results were used to accurately determine the primary PRN codes by averaging over many code periods. The resulting PRN codes can be obtained on-line at http://gps.ece.cornell.edu/galileo/. This paper explains how the codes were determined.

The remainder of this paper is divided into 3 sections plus conclusions. Section II describes the codeless acquisition scheme that was used to determine the signal's carrier frequency and phase along with its BOC phase. Section III describes how base-band 1.023-MHz accumulations were computed and then used to determine the GIOVE-A PRN codes. Section IV briefly describes the characteristics of the GIOVE-A signal. Section V presents the paper's conclusions.

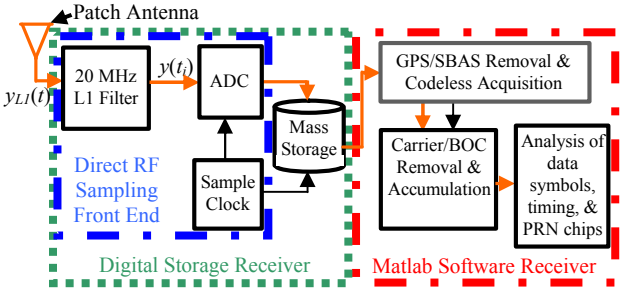

Fig. 1. Schematic block diagram of the data recording hardware and the post-processing software receiver.

II. CODELESS SIGNAL ACQUISITION

A. Signal Modal

The analysis has required a detailed understanding of the Galileo L1 signal structure. A coherent signal description was pieced together from early, publicly available drafts of the Galileo ICD and other documentation [1,2]. Later findings demonstrated that these documents are generally accurate, with a few important exceptions. In this section, the GIOVE-A L1 BOC(1,1) signal structure is presented as the authors currently understand it.

The BOC(1,1) signal is composed of two multiplexed channels: the L1-B data channel and the L1-C pilot channel. The sampled Galileo L1 BOC(1,1) signal that exits the RF front-end of Fig. 1 takes the form

$$y_i = A\,[b_{L1\text{-}B}(t_i)d_{L1\text{-}B}(t_i) - c_{L1\text{-}C}(t_i)s_{L1\text{-}C}(t_i)]\,s_{SC}(t_i) \times \cos(2\pi f_{IF}t_i + f_0) + n_i \qquad (1)$$

at receiver sample time t_i. The quantities in Eq. (1) are the carrier amplitude A, the PRN code of the data channel $b_{L1\text{-}B}(t_i)$, the data symbol values $d_{L1\text{-}B}(t_i)$, the primary PRN code of the pilot channel $c_{L1\text{-}C}(t_i)$, the secondary code of the pilot channel $s_{L1\text{-}C}(t_i)$, the sine-phased BOC signal $s_{SC}(t_i) = sign[\sin(2\pi f_{BOC}t_i)]$ with nominal BOC frequency $f_{BOC} = 1.023\times10^6$ Hz, the intermediate value of the nominal f_{L1} carrier frequency f_{IF}, the initial carrier phase f_0, the measurement noise n_i, and the broadcast time

$$t_i = t_0 + (t_i\text{-}t_0)[1 + w_{D0}/(2\pi f_{L1})] + (t_i\text{-}t_0)^2[0.5a_D/(2\pi f_{L1})] \qquad (2)$$

This formula for the broadcast time accounts for the effects of the initial carrier Doppler shift w_{D0} and the carrier Doppler shift rate a_D on the received frequencies of the data bits, the PRN code chips, and the BOC.

The PRN codes and the data time history in Eq. (1) take the form

$$b_{L1\text{-}B}(t_i) = \sum_{n=-\infty}^{\infty} b_{mod(n,4092)}P_{T_c}(t_i\text{-}nT_c) \qquad (3a)$$

$$d_{L1\text{-}B}(t_i) = \sum_{n=-\infty}^{\infty} d_n P_{T_d}(t_i\text{-}nT_d) \qquad (3b)$$

$$c_{L1\text{-}C}(t_i) = \sum_{n=-\infty}^{\infty} c_{mod(n,8184)}P_{T_c}(t_i\text{-}nT_c) \qquad (3c)$$

$$s_{L1\text{-}C}(t_i) = \sum_{n=-\infty}^{\infty} s_{mod(n,25)}P_{T_s}(t_i\text{-}nT_s) \qquad (3d)$$

where b_0, ..., b_{4091} is the PRN code of the L1-B data channel, ..., d_0, d_1, d_2, ... is the navigation data symbol sequence, c_0, ..., c_{8183} is the primary PRN code for the L1-C pilot channel, and s_0, ..., s_{24} is the secondary PRN code for the pilot channel. The sequence elements take on +1/-1 values. The function $P_T(t)$ is the usual rectangular support function, which is equal to one over the interval $0 = t < T$ and zero elsewhere.

The goal of this project has been to determine the three PRN code sequences b_0, ..., b_{4091}, c_0, ..., c_{8183}, and s_0, ..., s_{24}. The nominal chipping/symbol rates for these sequences are $1/T_c$ = 1.023 MHz for the L1-B PRN code and the L1-C primary PRN code, $1/T_d$ = 250 Hz for the L1-B data symbols, and $1/T_s$ = 125 Hz for the L1-C secondary PRN code. The L1-B PRN code has a nominal period of 4 ms. The combined L1-C PRN code has a nominal period of 200 ms. A graphical representation of the data symbols and PRN codes is given in Figure 2.

B. Signal Acquisition Statistic

The signal has been acquired by maximizing a codeless acquisition statistic. This statistic has been computed based on 2 types of in-phase and quadrature accumulations. Accumulations of the first type have been computed after mixing to baseband using a replica of the BOC signal and a replica of the in-phase or quadrature carrier signal:

$$I_j(t_0,w_{D0},a_D) = \sum_{i=i_j}^{i_{j+1}-1} y_i s_{SC}(t_i)\cos(2\pi f_{IF}t_i) \quad \text{for } j = 0, ..., J\text{-}1 \qquad (4a)$$

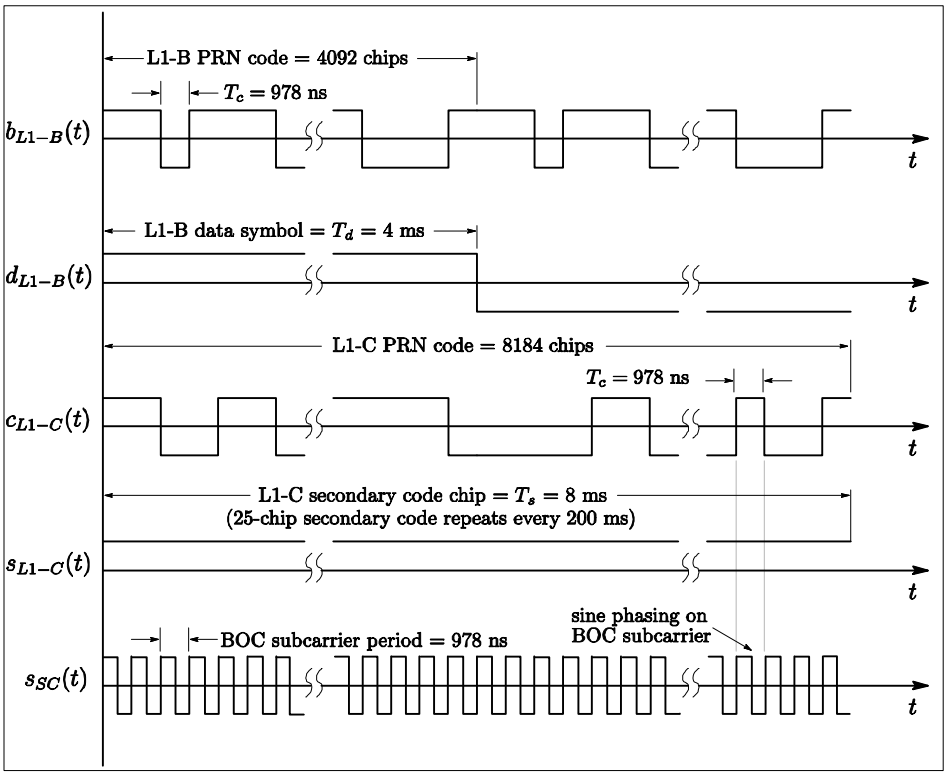

Fig. 2. Timing diagram of components of GIOVE-A L1 BOC(1,1) signal.

$$Q_j(t_0,w_{D0},a_D) = \sum_{i=i_j}^{i_{j+1}-1} y_i s_{SC}(t_i) sin(2\pi f_{IF} t_i)$$
$$\text{for } j = 0, ..., J\text{-}1 \qquad (4b)$$

The BOC phase t_0, the Doppler shift w_{D0}, and the Doppler shift rate a_D have been used implicitly in this calculation because they affect the computation of the broadcast sample time t_i as a function of the received sample time t_i as defined in Eq. (2). The accumulations have been computed at the nominal 1.023 MHz chipping rate of the L1-B and L1-C PRN codes. They have been aligned with the j^{th} chip interval as defined by the non-zero portion of the function $P_{T_c}(t_i\text{-}jT_c)$ that appears in the summations of Eqs. (3a) and (3c). Thus, i_j is the minimum value of i such that $j \le 1.023\times10^6 t_i$.

The accumulations of the second type have been defined to exploit the observed 200 ms periodicity of the total L1-C pilot PRN code. These latter accumulations are sums of accumulations from Eqs. (4a) and (4b):

$$I_{Cj}(t_0,w_{D0},a_D) = \sum_{k=0}^{K-1} I_{[j+204600k]}(t_0,w_{D0},a_D)$$
$$\text{for } j = 0, ..., 204599 \qquad (5a)$$

$$Q_{Cj}(t_0,w_{D0},a_D) = \sum_{k=0}^{K-1} Q_{[j+204600k]}(t_0,w_{D0},a_D)$$
$$\text{for } j = 0, ..., 204599 \qquad (5b)$$

The number of elements in each sum is $K = floor(J/204600)$. This is the number of full 200 ms periods of the total L1-C PRN code for which accumulations have been computed in Eqs. (4a) and (4b). These new accumulations can be used to increase the signal detection power of the acquisition along with its sensitivity to carrier Doppler shift.

A locally-most powerful Neyman-Pearson-type acquisition statistic [3] has been developed using the accumulations in Eqs. (4a)-(5b). The original acquisition statistic depended on the unknown signal parameters t_0, w_{D0}, a_D, f_0, and A. Development of a locally-most-powerful statistic eliminates the amplitude dependence by computing the statistic in the limit as A approaches 0 [3]. Analytic optimization with respect to the initial carrier phase f_0 eliminates one more unknown parameter. Optimization of f_0 makes the statistic slightly sub-optimal for signal detection purposes, which seems counter-intuitive, but this optimization is believed to further increase the statistic's sensitivity to carrier Doppler shift w_{D0}. The resulting codeless acquisition statistic is

$$g(t_0,w_{D0},a_D) = \tfrac{1}{2}[a + c + \sqrt{4b^2 + (a-c)^2}] \qquad (6)$$

where the parameters a, b, and c are computed from the accumulations in Eqs. (4a)-(5b):

$$a = \sum_{j=0}^{J-1} I_j^2(t_0,w_{D0},a_D) + \sum_{j=0}^{204599} I_{Cj}^2(t_0,w_{D0},a_D) \qquad (7a)$$

$$b = \sum_{j=0}^{J-1} I_j(t_0,w_{D0},a_D) Q_j(t_0,w_{D0},a_D) + \sum_{j=0}^{204599} I_{Cj}(t_0,w_{D0},a_D) Q_{Cj}(t_0,w_{D0},a_D) \qquad (7b)$$

$$c = \sum_{j=0}^{J-1} Q_j^2(t_0,w_{D0},a_D) + \sum_{j=0}^{204599} Q_{Cj}^2(t_0,w_{D0},a_D) \qquad (7c)$$

The corresponding optimal estimate of the initial carrier phase is $f_{0opt} = \frac{1}{2} atan2[-2b,(a-c)]$.

C. Search Strategy

The search for the GIOVE-A signal has determined t_0, w_{D0}, and a_D values that maximize $g(t_0,w_{D0},a_D)$. The search has used the NORAD tracking ephemerides for GIOVE-A in order to determine a reasonable value for the Doppler shift rate value a_D and a range of possible values for the initial Doppler shift w_{D0}. The search has covered one BOC period of possible t_0 values, i.e. 1/(1.023 MHz) = 977.517 ns. The search has been conducted on a grid in (t_0,w_{D0}) space. The t_0 granularity of the search grid has been set to be about 0.1 BOC period, and the granularity of the w_{D0} search grid has been set to be approximately $2.5p/K$ rad/sec. This grid spacing ensures that the peak phase error due to Doppler shift error will be below $p/4$ radians over the entire data batch.

The search has started with a coarse phase and has finished with a fine phase. The coarse search has been designed to execute more rapidly by using a reduced number of accumulations and a reduced number of frequency grid points because it is based on data from a single L1-C code period (i.e., $K = 1$). The Doppler shift determined by the coarse phase has provided a starting point for a fine search that has searched over a smaller span of Doppler-shift uncertainty using an acquisition statistic that has been computed over a larger number of L1-C code periods. The added data in this search and its finer frequency grid have combined to yield an accurate estimate of the received carrier phase time history.

D. Removal of GPS and SBAS Signals Prior to GIOVE-A Signal Processing

GPS and SBAS C/A-code signals can interfere with codeless acquisition and analysis of the Galileo L1 BOC(1,1) signal. C/A-code signals produce significant power in the accumulations of Eqs. (4a) and (4b) when their chip transition times occur halfway through an accumulation interval. This happens because changes of their chip values mix with the sine-phased BOC signal to produce non-zero averages.

Interference from GPS and SBAS signals has been eliminated by tracking these signals and removing them from the data. This process is illustrated by the power spectrum in Fig. 3. The raw recorded data from the digital storage receiver has been used to acquire, track, and remove all GPS and SBAS signals in view. The power spectral density of the raw data in Fig. 3 clearly shows a central hump caused by the GPS and SBAS signals. The original hump disappears after removal of these signals, revealing two distinct lobes to each side of the intermediate frequency. These two humps constitute the expected signature of the GIOVE-A L1 BOC(1,1) signal.

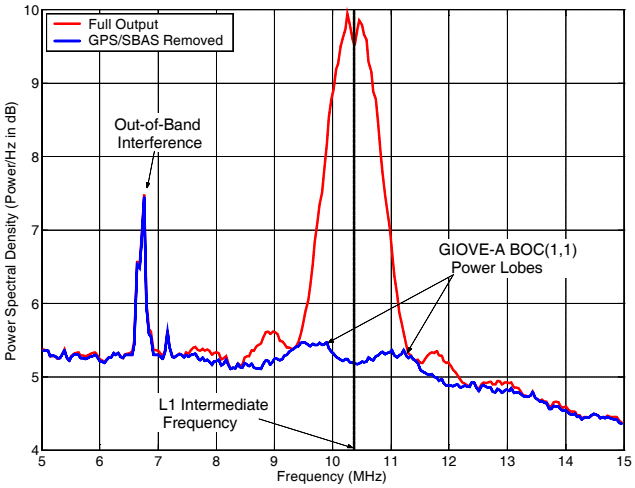

Fig. 3 L1-band power spectral densities: raw data and data after removal of GPS and SBAS L1 C/A-code signals.

E. GIOVE-A BOC(1,1) Acquisition Results

The acquisition procedure has been applied to data that were recorded on 2 March 2006 and on 8 March 2006. The two data sets were taken when GIOVE-A was visible both from Ithaca and from Europe during European business hours -- a measure taken to increase the likelihood that the satellite was broadcasting. The flyovers were predicted using NORAD elements. Figure 4 presents the results of a fine acquisition that has been based on 1 second of data from March 8th. It is a 2-dimensional plot of the Eq.-(6) g vs. t_0 and w_{D0}. The plot's distinct peak indicates that the GIOVE-A signal is present. The signal's BOC phase and Doppler shift have been determined from their values at the peak.

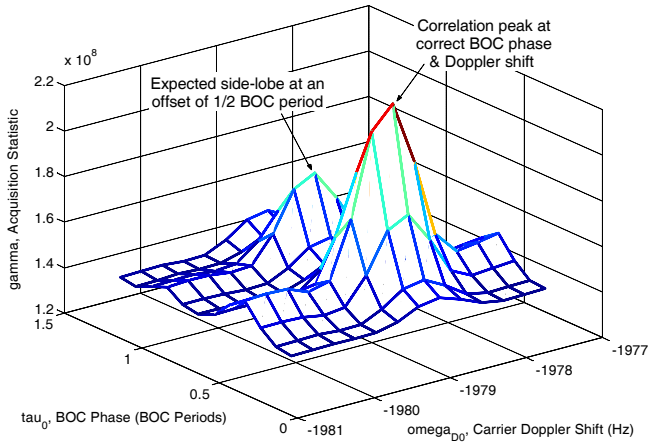

Fig. 4. Fine-scale estimation of BOC phase and Doppler shift based on the codeless acquisition statistic.

III. CODE BREAKING

Removal of the carrier and the BOC modulation leaves a signal whose only components are the PRN codes and noise. Derivation of this signal is the next step.

A. In-Phase Accumulations

The signal that contains the PRN codes has been derived by computing 1.023 MHz base-band accumulations that are in-phase with the estimated carrier signal. The original 1.023 MHz in-phase and quadrature accumulations from Eqs. (4a) and (4b) have been rotated by the optimal initial carrier phase f_{0opt} in order to produce the new in-phase accumulations:

$$I_j^f = \cos f_{0opt}\, I_j(t_{0opt}, w_{D0opt}, a_{Dopt}) - \sin f_{0opt}\, Q_j(t_{0opt}, w_{D0opt}, a_{Dopt}) \quad \text{for } j = 0, \ldots, J\text{-}1 \tag{8}$$

The $()_{opt}$ subscript denotes the values associated with the acquisition peak in Fig. 4. The $()^f$ superscript indicates that the f_{0opt} rotation has been applied.

An early indication of the presence and structure of the GIOVE-A signal came from a plot of the circular autocorrelation function of the I_j^f accumulations, which is shown in Figure 5 for a 2-second batch of data from March 8th. Its high central peak at zero delay is mainly the result of a powerful noise component -- the SNR of the accumulations is -4.7 dB. The secondary peaks at multiples of 200 ms are caused by the L1-C pilot signal. Many of the smaller peaks between the 200 ms peaks occur at regular intervals of 4 ms, i.e., at the period of the L1-B PRN code.

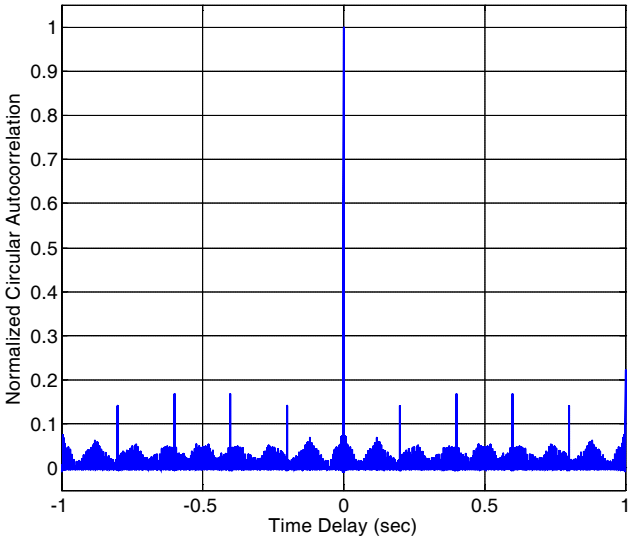

Fig. 5. Normalized circular autocorrelation of GIOVE-A 1.023 MHz in-phase accumulations.

The peaks at 200 ms intervals were a surprise. Prior to seeing this plot, the authors had learned from Galileo documentation that the L1-C PRN code period was 100 ms, but these peaks clearly indicated a 200 ms period. The positive values of the smaller peaks that were separated by 4 ms was a second surprise. This sign constancy indicated that the L1-B data bits were primarily of a single sign.

B. Approximate PRN Code Timing

The first step in determining the PRN code chips from the I_j^f accumulations has been to approximately estimate the start/stop times of L1-B PRN code periods. This has been accomplished by using a differential analysis to look for times of probable data symbol transitions on the L1-B signal. This analysis has computed the following differential time history:

$$D_\ell = \sum_{j=\ell}^{\ell+4091} (I_j^f - I_{j+4092}^f)^2 \quad \text{for } \ell = 0, \ldots, L\text{-}1 \tag{9}$$

A plot of D_ℓ vs. ℓ will have a high value if ℓ is the accumulation index of the first chip of an L1-B PRN code period and if the two successive L1-B data symbols that start at indices ℓ and ℓ +4092 have opposite signs. Conversely, this plot will take on a low value at the start of a pair of PRN code periods that have equal data symbol signs. Noise makes it impossible to exactly determine the initial sample time of a code period based on a D_ℓ vs. ℓ plot, but the occurrence of several peaks and dips at multiples of 4092 accumulations will yield a rough estimate of the L1-B PRN code timing.

Consider the plot of D_ℓ vs. ℓ/4092 in Fig. 6, which is based on 204 ms of data from 8 March 2006. The plot has 4 sharp peaks at ℓ/4092 ≅ 27.05, 29.08, 33.03, and 35.06. It has two sharp dips at ℓ/4092 ≅ 28.07 and 34.04. The average of the fractional parts of these ℓ/4092 values can be multiplied by 4092 in order to form an approximate estimate of the initial sample index of the first L1-B PRN code period. This estimate is ℓ_{app} = 224. Later results have indicated that this approximation's error is less than 1% of a code period. Note that the plateaus in Fig. 6 correspond to periods of prolonged constancy or prolonged alternating variation of the L1-B data symbol signs.

C. Determination of Data Symbols and Secondary Code Chips

The next step in unraveling the PRN codes is to determine the L1-B data symbol time history d_0, d_1, d_2, ... and the L1-C secondary code time history s_0, ..., s_{24}. The I_j^f accumulations and the approximate times of the L1-B PRN code periods can be used to determine the +1/-1 values for these quantities.

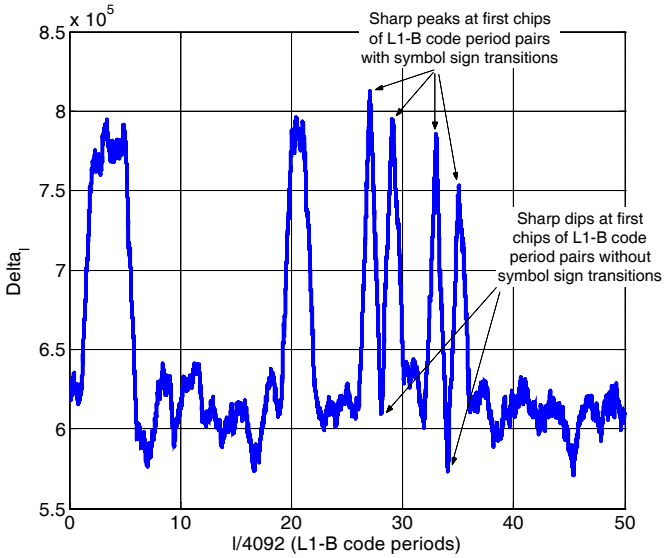

Fig. 6. PRN code period differential timing statistic as a function of 1.023 MHz sample number.

Let the m^{th} approximate L1-B code period consist of the accumulations with indices $j_m = \ell_{app}+4092m$ to $j_{m+1}-1 = \ell_{app}+4092(m+1)-1$. The determination of L1-B symbols and L1-C secondary code chips starts with a determination of "soft" linear combinations of these unknowns:

$$U_m = \sum_{Dj=0}^{4091} I^f_{[\ell_{app}+Dj]} I^f_{[\ell_{app}+Dj+4092m]} \quad \text{for } m = 1, \ldots, M\text{-}1 \qquad (10)$$

U_m is the cross correlation between the 1.023 MHz accumulations of the 0^{th} L1-B PRN code period and those of the m^{th} code period. The maximum number of such cross correlations is $M\text{-}1 = floor[(J\text{-}\ell_{app})/4092] - 1$.

If there were no noise in the accumulations and if the carrier amplitude were constant, then the computed U_m values would take on 5 possible levels: $-U_{nom}$, $-0.5U_{nom}$, 0, $+0.5U_{nom}$, and $+U_{nom}$. The values $-U_{nom}$, 0, and $+U_{nom}$ occur when m is even, and the values $-0.5U_{nom}$ and $+0.5U_{nom}$ correspond to odd values of m. $U_m \cong +U_{nom}$ implies that the L1-B data symbol and the L1-C secondary code chip both have the same sign as they have when $m = 0$. $U_m \cong -U_{nom}$ implies that they both have the opposite signs, and $U_m \cong 0$ occurs when one has the same sign and the other has the opposite sign. Similarly, $U_m \cong +0.5U_{nom}$ implies that the L1-B data symbol has the same sign as when $m = 0$, and $U_m \cong -0.5U_{nom}$ implies that it has the opposite sign. Nothing can be said about the L1-C secondary code chips for these odd-m cases because the $m = 0$ case corresponds to a different half of the L1-C primary code than do the cases $m = 1, 3, 5, \ldots$

The indeterminate $U_m \cong 0$ cases are resolved by computing new correlations with the 1.023 MHz accumulations from one of these cases:

$$V_m = \sum_{Dj=0}^{4091} I^f_{[\ell_{app}+Dj+4092m_z]} I^f_{[\ell_{app}+Dj+4092m]}$$
$$\text{for } m = 1, \ldots, M\text{-}1, \; m \neq m_z \qquad (11)$$

where m_z is one of the even-valued correlation indices that yields $U_{m_z} \cong 0$. These new correlations also take on the approximate values $-U_{nom}$, $-0.5U_{nom}$, 0, $+0.5U_{nom}$, and $+U_{nom}$.

A plot of the V_m correlations vs. the U_m correlations can be used to determine the L1-B data symbols and half of the L1-C secondary code chips, as in Fig. 7. The figure's blue points correspond to even values of m and yield fully determined L1-B symbol signs and L1-C secondary PRN code chip signs. The red points, which correspond to odd-valued m, yield L1-B symbol signs, but the L1-C secondary PRN code chips are undetermined. The symbol/chip sign determinations are made using the discriminator lines shown in the figure. Note that the nominal correlation magnitude for this figure is $U_{nom} \cong 50000$.

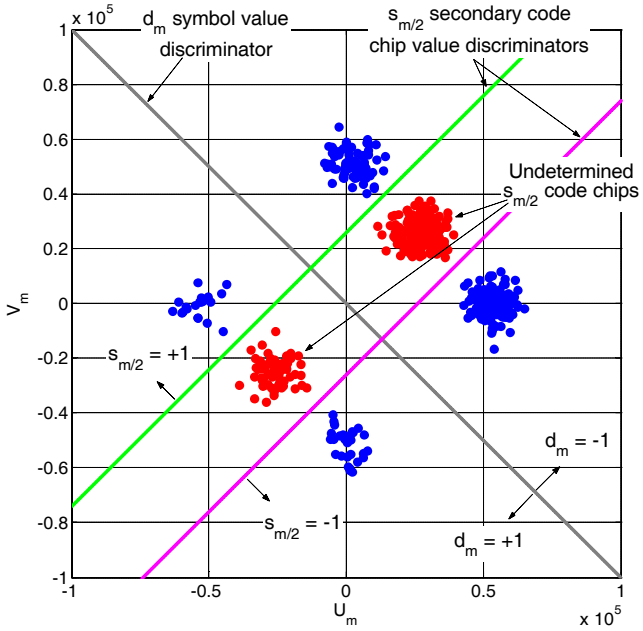

Fig. 7. Determination of L1-B data symbols and L1-C secondary PRN code chips based on "soft" linear combinations as computed by correlation analysis, 2 March 2006 data.

The undetermined L1-C secondary code chip values can be resolved by performing a similar analysis that reverses the roles of the even and odd indices. It starts with a modified version of Eq. (10) that replaces $I^f_{[\ell_{app}+Dj]}$ by $I^f_{[\ell_{app}+Dj+4092]}$. This new analysis re-confirms the L1-B symbol signs, and it produces a sequence of L1-C

secondary code chips for the odd-m code periods. These new chips are identical to the chips produced by the even-m analysis, except that they have an offset either one index ahead or one index behind the even-m chip sequence. Thus, no new information about the +1/-1 values of the s_j secondary L1-C code chips is obtained. Rather, the new information concerns whether the 8 ms L1-C primary PRN code periods line up with the pairs of 4 ms L1-B data bits (d_0, d_1), (d_2, d_3), (d_4, d_5), ... or with the pairs (d_1, d_2), (d_3, d_4), (d_5, d_6), ...

The data symbols and the secondary code chips determined by this analysis constitute the sequences d_0, d_1, d_2, ..., d_{M-1} and s_0, s_1, s_2,..., $s_{(M-2)/2}$ that appear in Eqs. (3b) and (3d). The values of d_0 and s_0 are assigned to be +1 in order to be consistent with the above analysis. As a check, one can verify that the L1-C secondary PRN code satisfies the 25-chip periodicity condition: $s_p = s_{p+25}$. Note that these values have a sign ambiguity; i.e., d_0, d_1, d_2, ..., d_{M-1} may all change sign together, and s_0, s_1, s_2,..., $s_{(M-2)/2}$ may do the same. The possibility of a sign reversal is caused by a 180 deg carrier phase ambiguity. An additional ambiguity is that the true start chip of the L1-C secondary code sequence could be any of its 25 chips. For example, the Galileo program may consider the true sequence to be s_7, ..., s_{24}, s_0, ..., s_6.

Blind Alleys. The project went down three blind alleys on its way to determining the d_0, d_1, d_2, ..., d_{M-1} and s_0, s_1, s_2,..., $s_{(M-2)/2}$ values. The first wrong conjecture was that the L1-C primary code maintained a length of 4092 chips and that its 200 ms period was caused by a lengthening of the secondary code from 25 chips to 50 chips. Under thus assumption, there would be 50 L1-C secondary PRN code chips to be determined: s_0, ..., s_{49}.

This wrong assumption and some additional analysis indicated that there should be 3 possible nominal levels of U_m: $-U_{nom}$, 0, and $+U_{nom}$. The actual data showed the 5 nominal levels: U_{nom}, $-0.5U_{nom}$, 0, $+0.5U_{nom}$, and $+U_{nom}$.

This discrepancy led to the second wrong conjecture: that the signal contained four 4092-chip PRN codes and that each of these codes carried one data symbol or one secondary code chip per period. This conjecture explained the 5 nominal levels of U_m. It was tested by computing the V_m values defined in Eq. (11) and by making the plot shown in Fig. 7. Note how the points on the plot are organized into groups at the vertices of a diamond and at the centers of two of its sides. The lengths of the diagonals of this diamond are $2U_{nom} \cong 10^5$. If the four-code hypothesis had been correct, then there should have been three additional groups of points, one at the origin and two at the centers of the other two sides of the diamond.

The Fig.-7 plot caused the 4-codes conjecture to be discarded, but it led to a third wrong conjecture: that the s_m secondary code chips could take on 3 values: -1, 0, and +1. The red points on Fig. 7 seemed to correspond to zero values. Armed with this hypothesis, the lines shown on Fig. 7 were used to discriminate the d_m data symbol values and the s_m secondary code chip values. It was found that the s_m chips did have a periodicity of 50, i.e., $s_m = s_{m+50}$. It was also found that the zero-valued s_m chips were the odd chips, i.e., $0 = s_1 = s_3 = s_5 = ...$

Although this hypothesis was wrong, it was completely consistent with the data, and it allowed the determination of the entire L1-B PRN code and half of the L1-C primary PRN code. The error in this hypothesis was not discovered until after the initial publication of the PRN codes. In response, a colleague forwarded a pre-print of Ref. [4] to the authors. Reference 4 demonstrates that the primary L1-C PRN code is 8184 chips long rather than 4092 chips long and that the L1-C secondary code is 25 chips long with no zero-valued chips. In hindsight, the authors should have realized this fact because the existence of zero-valued chips would have had severe negative ramifications for the ability of the GIOVE-A L1 transmitter to maintain a constant carrier power level.

D. Determination of Primary PRN Code Chips

The L1-B PRN code, the L1-C primary PRN code, and the PRN code timing have been determined simultaneously by solving a maximum a posteriori estimation problem. Suppose, without loss of generality, that the already determined L1-B data symbols d_{2p} and d_{2p+1} correspond to the same 8 ms as the L1-C secondary code chip s_p for all p = 0, 1, 2, ..., (M-2)/2. Then minimization of the following re-scaled negative-log-likelihood cost function yields the maximum a posteriori estimates of the L1-B code chips b_0, ..., b_{4091}, the L1-C primary code chips c_0, ..., c_{8183}, the accumulation amplitude A_I, and the code start-time index, m:

$$\boldsymbol{b} = \frac{1}{2}\sum_{Dj=0}^{4091}\sum_{p=0}^{(M-2)/2}\left\{[I^f_{(m+Dj+8184p)} - A_I(b_{Dj}\,d_{2p} - c_{Dj}\,s_p)]^2 + [I^f_{(m+Dj+4092+8184p)} - A_I(b_{Dj}\,d_{2p+1} - c_{Dj+4092}\,s_p)]^2\right\} \quad (12)$$

This cost function amounts to a sum of the squared errors between the in-phase accumulations computed in Eq. (8) and modeled values of these accumulations that can be derived from Eqs. (1)-(4b) and (8).

The $\boldsymbol{b}$ cost function in Eq. (12) can be minimized by using a mixed integer/real optimization scheme. A brute-force outermost integer optimization searches over every m in a range of possible values near ζ_{app} -- recall that ζ_{app} is the rough approximation of the code start index. For each fixed m value in this range, $\boldsymbol{b}$ is minimized in an

intermediate real-valued optimization of the amplitude A_I that is wrapped around an inner minimization with respect to b_0, ..., b_{4091} and c_0, ..., c_{8183}. The latter minimization is accomplished by brute-force consideration of all possible +1/-1 combinations of the chip values. This inner minimization is simplified by the following fact: The cost terms that depend on each 3-tuple [b_j, c_j, c_{j+4092}] are independent of all of the other cost terms if A_I is held fixed. Therefore, each set of cost terms can be minimized by considering only $2^3 = 8$ different chip combinations. The cost function for the intermediate A_I optimization is piece-wise quadratic in A_I, and it can be minimized by using a Newton-like method [5].

This optimal estimation problem has been solved twice using independent 2-second data sets, one from 2 March 2006 and one from 8 March 2006. Figure 8 shows the outermost optimization of b as a function of m for the March 8th data. It is obvious from the figure that the code start time has a unique optimum. The optimal PRN codes have been found to be identical for the two data sets. As with the L1-B data symbols and the L1-C secondary code chips, these code chips have a sign ambiguity so that b_0, ..., b_{4091} can all change sign together as can c_0, ..., c_{8183}.

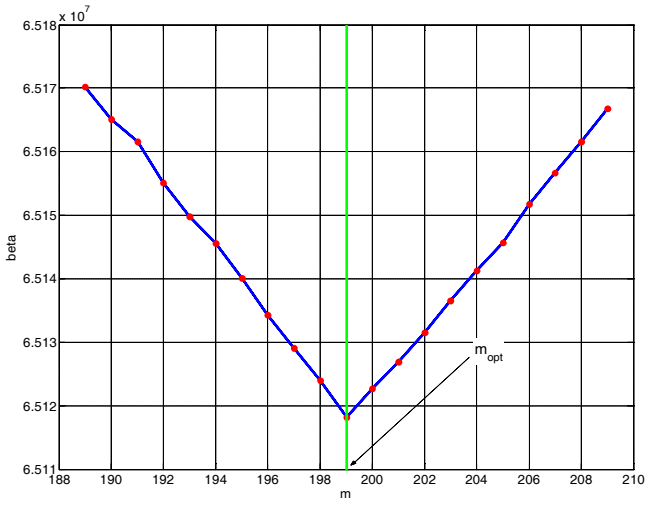

Fig. 8. Dependence of cost b on PRN start time m after optimization of PRN code chips and accumulation amplitude.

A conservative method has been used to evaluate the probability of a chip error in the determined PRN codes. This method solves for "soft" values of the PRN code chips by treating the quantities $A_I b_0$, ..., $A_I b_{4091}$ and $A_I c_0$, ..., $A_I c_{8183}$ as real-valued unknowns and by minimizing the b cost function with respect to these unknowns using linear least-squares techniques [5]. The signs of the resulting values equal the integer-valued chip estimates from the mixed integer/real optimization. The distributions of these values' magnitudes can be used to estimate the probability of a chip sign error due to random noise effects. This probability is less than 8.5×10^{-11}; the chip estimates are highly reliable.

IV. GIOVE-A L1 BOC(1,1) SIGNAL PROPERTIES

The PRN codes have been used to determine that the GIOVE-A signal behaves nominally. For example, Fig. 9 compares the experimentally determined shape of the L1-B PRN code's correlation function with its theoretical shape. The blue curve has been computed by correlating a replica PRN code with measured in-phase data from 100 code periods. The green-dotted theoretical curve is very closely aligned with the blue experimental curve. The red curve shows the correlation between the replica PRN code and the measured quadrature signal. This latter correlation is nearly zero, as it should be.

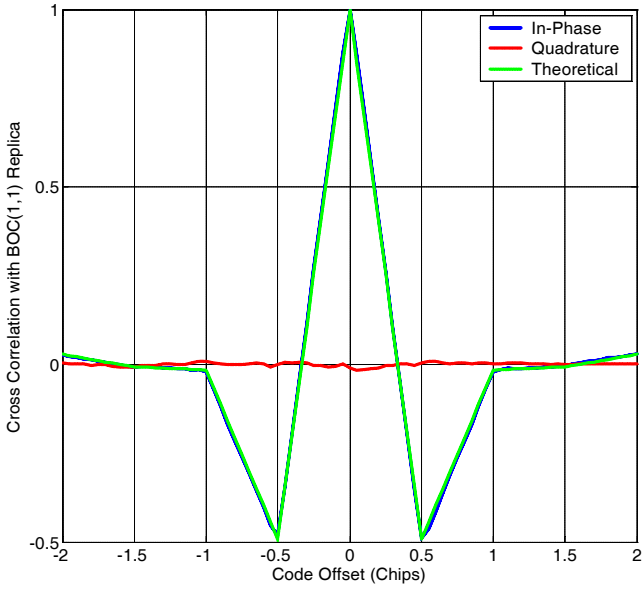

Fig. 9. Comparison between theoretical and experimental L1-B PRN code correlation functions

Additional GIOVE-A signal properties are as follows: The signal power has been found to be about 5.8 dB weaker than the strongest GPS L1 C/A-code signals when GIOVE-A is at a 45 deg elevation. The measured Doppler shift has been found to be within 10 Hz of the expected value based on NORAD data, which is within the margin of error of the receiver clock and the NORAD ephemerides.

V. SUMMARY AND CONCLUSIONS

A method has been developed for determining the PRN codes of a Galileo satellite's L1 BOC(1,1) signal. This method involves codeless acquisition, computation of 1.023 MHz baseband in-phase accumulations, and analysis of these accumulations to determine PRN code

start times and chip values. These techniques have been applied to GIOVE-A data collected using a patch antenna and a digital storage receiver. The PRN codes have been determined independently from two sets of 2-second data batches that were recorded 6 days apart from each other. The resulting PRN codes are identical, and the error probability of each chip is less than 8.5×10^{-11}. Subsequent analysis of the GIOVE-A signal has determined that it has power levels about 6 dB lower than the strongest GPS L1 C/A signals and that its structure has the expected properties of a BOC(1,1) signal.

ACKNOWLEDGEMENTS

This work has been supported in part by the NASA Office of Space Science through grant No. NNX06AC34G. Madhulika Guhathakurta is the grant monitor.

REFERENCES

1. Hein, G.W., Godet, J., Issler, J.-L., Martin, J.-C., Erhard, P., Lucas-Rodriguez, R., and Pratt, T., "Status of Galileo Frequency and Signal Design", *Proc. ION GPS 2002*, Portland, OR, 24-27 Sept. 2002, pp. 266-277.
2. Anon., "L1 Band Part of Galileo Signal in Space ICD (SIS ICD)", Galileo Joint Undertaking, Tdoc G2-050266, available on-line at: http://www.galileoju.com/doc/Galileo%20standardisation%20document%20for%203GPP.pdf, Quebec, Canada, 23-27 May 2005.
3. Poor, H.V., *An Introduction to Signal Detection and Estimation*, Springer-Verlag, (New York, 1988), pp. 31-36, 53-54.
4. Montenbruck, O., Günther, C., Graf, S., Garcia-Fernandez, M., Furthner, J., and Kuhlen H., "GIOVE-A Initial Signal Analysis", *GPS Solutions*, Vol. 10, No. 2, May 2006, pp. 146-153.
5. Gill, P.E., Murray, W., and Wright, M.H., *Practical Optimization* Academic Press, (New York, 1981), pp. 37-40, 105-111.